

AD-A038 251

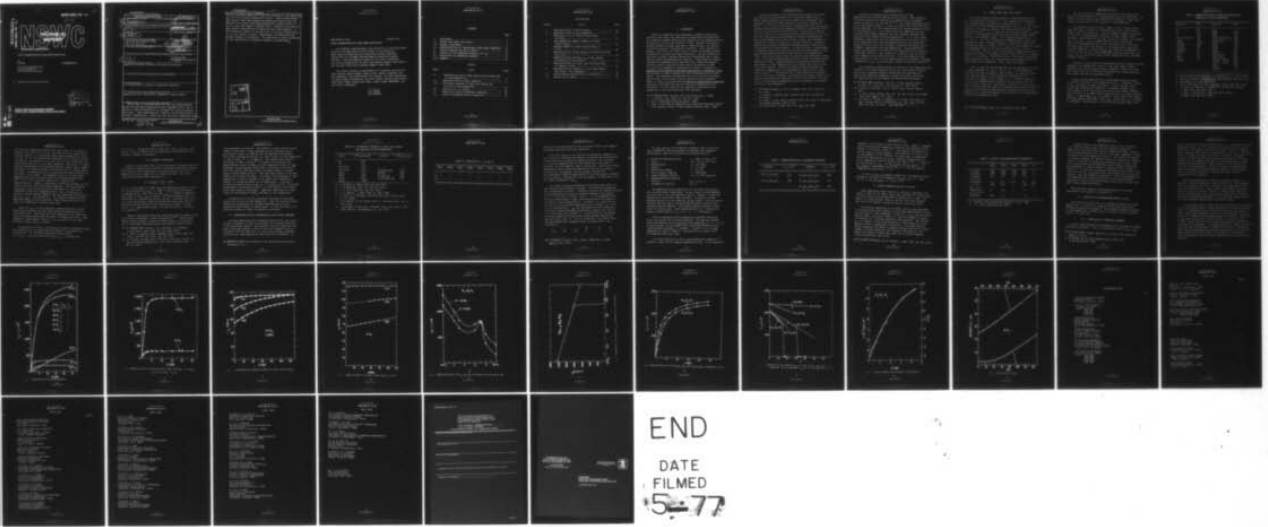
NAVAL SURFACE WEAPONS CENTER WHITE OAK LAB SILVER SP--ETC F/G 20/3
HIGHLY MAGNETOSTRICTIVE RARE EARTH-IRON ALLOYS.(U)
DEC 76 A E CLARK

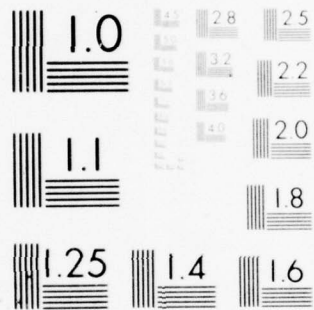
UNCLASSIFIED

NSWC/WOL/TR-76-99

NL

1 OF 1
AD
A038251





MICROCOPY RESOLUTION TEST CHART
NATIONAL BUREAU OF STANDARDS-1963-A

FG

NSWC/WOL/TR 76-99

12

ADA 038251
NSWC/WOL/TR 76-99

NSWC

TECHNICAL REPORT

WHITE OAK LABORATORY

HIGHLY MAGNETOSTRICTIVE RARE EARTH-IRON ALLOYS

BY
A.E. Clark

1 DECEMBER 1976

NAVAL SURFACE WEAPONS CENTER
WHITE OAK LABORATORY
SILVER SPRING, MARYLAND 20910

- Approved for public release; distribution unlimited

DDC
 RECEIVED
 APR 13 1977
 RECEIVED
 A

AD NO. _____
DDC FILE COPY

NAVAL SURFACE WEAPONS CENTER
WHITE OAK, SILVER SPRING, MARYLAND 20910

UNCLASSIFIED

SECURITY CLASSIFICATION OF THIS PAGE (When Data Entered)

REPORT DOCUMENTATION PAGE		READ INSTRUCTIONS BEFORE COMPLETING FORM
1. REPORT NUMBER 14 NSWC/WOL/TR-76-99	2. GOVT ACCESSION NO.	3. RECIPIENT'S CATALOG NUMBER 9
4. TITLE (and Subtitle) 6 Highly Magnetostrictive Rare Earth-Iron Alloys.	5. TYPE OF REPORT & PERIOD COVERED Technical report PERFORMING ORG. REPORT NUMBER	
7. AUTHOR(s) 10 A. E. Clark	8. CONTRACT OR GRANT NUMBER(s)	
9. PERFORMING ORGANIZATION NAME AND ADDRESS Naval Surface Weapons Center White Oak Laboratory White Oak, Silver Spring, Maryland 20910	17	10. PROGRAM ELEMENT, PROJECT, TASK AREA & WORK UNIT NUMBERS 61153N; 16 62762N; 62711N; RR02-206-01 RR02-206 WR3811;
11. CONTROLLING OFFICE NAME AND ADDRESS	11	12. REPORT DATE 1 December 1976
14. MONITORING AGENCY NAME & ADDRESS (if different from Controlling Office) 12 39p.	13. NUMBER OF PAGES 35	
	15. SECURITY CLASS. (of this report) Unclassified	
	15a. DECLASSIFICATION/DOWNGRADING SCHEDULE	
16. DISTRIBUTION STATEMENT (of this Report) Approved for public release; distribution unlimited		
17. DISTRIBUTION STATEMENT (of the abstract entered in Block 20, if different from Report)		
18. SUPPLEMENTARY NOTES To be published in Journal of Underwater Acoustics		
19. KEY WORDS (Continue on reverse side if necessary and identify by block number) Magnetostriction, Rare Earth, Transducer, Elastic Moduli		
20. ABSTRACT (Continue on reverse side if necessary and identify by block number) Since 1963, it has been known that the rare earth elements possess extraordinary magnetostrictions ($\approx 10,000 \times 10^{-6}$), far in excess of those characteristic of the magnetic transition metals and alloys. These magnetostrains, however, are available only at cryogenic temperatures. Within the last few years, magnetostrictive		

DD FORM 1473 1 JAN 73

EDITION OF 1 NOV 65 IS OBSOLETE S/N 0102-LF-014-6601

UNCLASSIFIED

SECURITY CLASSIFICATION OF THIS PAGE (When Data Entered)

391 596

Handwritten initials and a checkmark.

UNCLASSIFIED

.002500

SECURITY CLASSIFICATION OF THIS PAGE (When Data Entered)

strains exceeding 2500×10^{-6} have been achieved at room temperature in rare earth alloys containing Tb and Fe. These alloys possess the largest known room temperature magnetostrictions by far and maintain the largest known magnetomechanical coupling factor ($k = 0.6$) over wide ranges in applied field. Recently, both positive and negative magnetostrictive materials have been examined. In this technical report, an introduction to the highly magnetostrictive rare earths is given. Measurements on polycrystals and single crystals are presented. The importance of grain orientation in the fabrication of transducer elements is established.

ADDITIONAL	NAME	<input checked="" type="checkbox"/>
DATE	DATE	<input type="checkbox"/>
MANUFACTURER		<input type="checkbox"/>
JUSTIFICATION		
BY	DISTRIBUTION AVAILABILITY CODES	
Dist.	AVAIL.	SPECIAL
A		

UNCLASSIFIED

SECURITY CLASSIFICATION OF THIS PAGE (When Data Entered)

UNCLASSIFIED
NSWC/WOL/TR 76-99

NSWC/WOL/TR 76-99

1 December 1976

HIGHLY MAGNETOSTRICTIVE RARE EARTH-IRON ALLOYS

The research reported herein was carried out in the Solid State Branch of the Materials Division as part of the Office of Naval Research Magnetostrictive Materials Program (PO4-0081, NR 039-110) and the NSWC Advanced Magnetic Materials Program (IR-124). The development of materials for sonar transducers was jointly sponsored by the Naval Sea Systems Command (Code 06H1-2) and the Naval Electronics Systems Command (Code 3043).

The author gratefully acknowledges his coworkers, particularly Henry Belson, Howard Savage, James Cullen, Nobuaki Tamagawa, and Dale McMasters, who helped shape this program. He also acknowledges the many helpful discussions, with Earl Callen (American University), James Rhyne (NBS), Norman Koon (NRL), Robert Timme (NRL/USRD), and Jack Butler (Raytheon).

J. R. Dixon
J.R. DIXON
By Direction

CONTENTS

	Page
I. BACKGROUND.....	4
II. BINARY RARE EARTH IRON ALLOYS.....	7
III. MAGNETIC ANISOTROPY.....	13
IV. MAGNETOSTRICTION OF PSEUDOINARY LAVES PHASE COMPOUNDS...	14
V. ELASTIC ENERGIES AND THE ΔE EFFECT.....	20
VI. RESISTIVITY AND MAGNETORESISTANCE OF $Tb Fe_2$	22
VII. FABRICATION OF TRANSDUCER ELEMENTS.....	22
VIII. SUMMARY.....	24

Tables

Table	Title	Page
I.	Magnetostrictions of Some Polycrystalline Materials at Room Temperature.....	9
II.	Magnetostriction of RFe_2 Compounds.....	11
III.	Anisotropy Constants of some Cubic Metals and Ferrites at Room Temperature.....	15
IV.	Polarity of λ , K_1 and K_2	16
V.	Magnetostriction of Quaternary Compounds.....	19
VI.	Elastic and Magnetoelastic Properties.....	21

Illustrations

Figure	Title	Page
1	Magnetostriction of Tb-Fe Alloys.....	25
2	Magnetostriction of RFe ₂ Compounds.....	26
3	Magnetostriction of Single Crystal TbFe ₂ and ErFe ₂	27
4	Room Temperature Magnetic Moment of Single Crystal TbFe ₂	28
5	Magnetic Moment of Single Crystal ErFe ₂ at 4.2°K.....	29
6	Magnetostriction of Tb _{1-x} Dy _x Fe ₂ at Fields of 10 kOe and 25 kOe.....	30
7	Magnetostriction Constant λ_{111} of Tb _{1-x} Dy _x Fe ₂ determined by x-ray method.....	31
8	Magnetostriction of Tb _{.9} Pr _{.1} Fe ₂ and Tb _{.8} Pr _{.2} Fe ₂ vs. Magnetic Field.....	32
9	Magnetostriction Constant λ_{111} for some Ternary Rare Earth - Fe ₂ Compounds.....	33
10	Elastic Modulus and ΔE Effect in Terfenol-D.....	34
11	Resistivity of TbFe ₂	35

I. BACKGROUND

While the magnetostrictive phenomena of magnetic metals was known for many years, the importance of magnetostrictive materials as transducer elements dates to the discovery of the magnetostriction oscillator by Pierce¹ and Vincent² in 1928. Metallic transducers quickly emerged as cheap, high power, rugged devices, far superior to the then available piezoelectric materials. Their superiority, however, declined in the 1940's when an effort to develop synthetic piezoelectric crystals was highly successful. Barium titanate and the lead zirconate titanates emerged which possessed lower losses and far higher magnetomechanical coupling. These materials rapidly replaced the magnetostrictive materials even though the magnetostrictive metals remained the most robust and easiest to bond. In view of the advances in piezoelectric ceramics, a seminar on Magnetostrictive Materials and Their Application to Underwater Sound was convened in 1966 to assess the role of magnetostrictive transducers. The potential of magnetostrictive ferrites and transition metal alloys, such as Ni-Co, Fe-Co, and Fe-Al, were discussed.³ Again, in 1969, a workshop entitled Metallic Magnetoacoustic Materials was held to determine the state-of-the-art of magnetostrictive materials.⁴ At this time the low temperature magnetostrictive properties of the rare earths were just emerging.

1. G. Pierce, Proc. Am. Acad. Arts and Sciences 63, 1 (1928)
2. J. Vincent, Proc. Phys. Soc. 41, 477 (1929)
3. See J. Underwater Acoustics 17, 199 (1967)
4. Proc. of the Metallic Magnetoacoustic Materials Workshop, Edited by F. Gardner, Office of Naval Research, Boston, Mass. (1969)

Extensive research on the magnetostrictive properties of the rare earths was being carried out in the early 1960's at the Naval Ordnance Laboratory by Clark, Bozorth, and DeSavage⁵ and at Iowa State University (Ames Laboratory) by Alstad, Legvold and Rhyne⁶. At this time it was widely recognized that the rare earths possessed many extraordinary magnetic properties, properties attributed to the unfilled 4f electron shells. Of particular interest were the heavy rare earths metals, which crystallize into the h.c.p. structure and possess unusual magnetic ordering configurations. Huge atomic moments were found, as high as $10\mu_B$, which dwarfed the conventional values of $0.6\mu_B$ and $2.2\mu_B$ for Ni and Fe. Enormous magnetic anisotropies (difficulty of magnetization rotation) were also measured for these elements. In 1963 and 1964, a breakthrough in magnetostrictive materials occurred with the measurement of the basal plane magnetostrictions of Dy and Tb at low temperatures. These values still remain today the largest known magnetostrictions (~1%). The observed basal plane strains are 100x to 10,000x typical magnetostrictions. Enormous magnetic anisotropies inhibited the measurement of other magnetostriction constants and those of other rare earth elements. Efforts were made to understand both the temperature dependences of the magnetostrictions as well as their atomic origin.^{7,8} The application of these materials to magnetostriction vibrators, however, was severely restricted because of the relatively low ordering temperatures of the rare earths. Only Gd, which is essentially non-magnetostrictive, possesses a Curie point as high as room temperature.

5. A. Clark, R. Bozorth, and B. DeSavage, Phys. Rev. Letters 5, 100 (1963)
6. J. Alstad, S. Legvold, and J. Rhyne, Phys. Rev. Letters 10, 509 (1963)
7. N. Tsuya, A. Clark, and R. Bozorth, Proc. Int. Conf. on Magnetism, Nottingham, England, 1964, p. 250.
8. E. Callen and H. Callen, Phys. Rev. 129, 578 (1963)

A search for magnetostrictive materials with high magnetostriction at room temperature was started. Highly magnetostrictive rare earths Tb and Dy were combined with the magnetic transition metals: Ni, Co, and Fe.^{9,10} The largest magnetostriction by far was found in TbFe₂.¹¹ Of all the known rare earth-transition metal compounds, the iron compounds have the largest magnetostriction at room temperature. Of all rare earth-iron compounds, the rare earth-Fe₂ Laves phase compounds have the strongest exchange interactions and the highest ordering temperatures. It is this strong exchange, coupled with the high concentration of rare earth ions in these compounds which lifts the magnetostrictive and anisotropic properties of the rare earth elements, heretofore available only at cryogenic temperatures, to room temperature. Large magnetocrystalline anisotropies ($>10^7$ ergs/cm³) and magnetostriction constants (>2000 ppm) persist in these compounds in spite of the high cubic point symmetry at the rare earth site. This high symmetry effectively shorts out one of the two magnetostriction constants, yielding a spectacular $\lambda_{111} \gg \lambda_{100}$ anisotropy, unknown in any other material.¹²

This technical report presents an overview of the magnetostriction studies of the highly magnetostrictive rare earth alloys, dealing with binary compounds, magnetic anisotropy, the importance of ternary and quaternary compounds, unusual ΔE effects, directions for improved material development and fabrication techniques.

9. A. Clark and H. Belson, 17th Conf. on Mag. and Mag. Mat'ls, Chicago, Ill., Nov 1971. See AIP Proc. 5, 1498 (1972)
10. N. Koon, A. Schindler, and F. Carter, Phys. Letters 37A 413 (1971)
11. A. Clark and H. Belson, Phys. Rev. B5, 3642 (1972); also IEEE Trans. Mag. MAG-8, 477 (1972)
12. A. Clark, J. Cullen, O. McMasters, E. Callen, 21st Conf. on Mag. and Mag. Mat'ls, Philadelphia, Pa., Dec. 1975; see AIP Conf. Proc. No. 29 (1976). Also NSWC/WOL/TR 75-177,

II. BINARY RARE EARTH IRON ALLOYS

The first compound found to exhibit a hugh magnetostriction at room temperature is $TbFe_2$.^{9,11} This compound still possesses the largest known room temperature magnetostriction. In Figure 1 is plotted the room temperature magnetostriction, $\lambda_{||} - \lambda_{\perp}$, vs. applied field for five Tb_xFe_{1-x} samples. All possess unusually large magnetostrictions. $(\lambda_{||} - \lambda_{\perp})$ denotes the fractional change in length parallel to the magnetic field minus the fractional change perpendicular to the magnetic field. (In nontextured materials, $\lambda_{||} - \lambda_{\perp} = \frac{3}{2} \lambda_s$). All three intermetallic compounds shown exhibit huge magnetostrictions: 194 ppm for Tb_2Fe_{17} , 1040 ppm for $TbFe_3$ and 2630 ppm for $TbFe_2$ at 25 kOe. For a 3 at % Tb in Fe sample (not shown) the magnetostriction is far from saturation with $(\lambda_{||} - \lambda_{\perp})/H = 6.5 \times 10^{-10}/Oe$. Both $Tb_{.03}Fe_{.97}$ and Tb_2Fe_{17} display large volume magnetostrictions. In $Tb_{.03}Fe_{.97}$, $\Delta V/VH = 88 \times 10^{-10}/Oe$, in Tb_2Fe_{17} , $\Delta V/VH = 37 \times 10^{-10}/Oe$. The Tb rich alloys, while also exhibiting large magnetostrictions, are substantially more rugged in the cast state than are the compounds: $TbFe_2$, $TbFe_3$ and Tb_2Fe_{17} .

Figure 2 shows the field dependence of the magnetostriction for the RFe_2 compounds ($R = Sm, Tb, Dy, Er, Tm$). The outstanding compounds are $TbFe_2$ and $SmFe_2$. They stand out as parallel giants with absolute values of room temperature magnetostriction >2000 ppm (for $SmFe_2$, $\lambda < 0$; for $TbFe_2$, $\lambda > 0$). This is because of: (1) the large magnetoelastic energy of the rare earth iron (Sm - most prolate in form; Tb - most oblate in form),^{7,13} and (2) the large iron-iron and rare earth-iron exchange constants which maintain the rare earth sublattice magnetization relatively intact at room temperature, so that the magnetostriction does not fall appreciably from its low temperature value.

13. K. W. H. Stevens, Phys. Soc. (London) 65, 209 (1952)

The slow increase in magnetostriction with field observed for DyFe_2 is representative of a large magnetocrystalline anisotropy. We show in the next section that indeed the anisotropy is large, with values of anisotropy $K \approx 10^7$ ergs/cm³ at room temperature.

The magnetostriction of ErFe_2 , TmFe_2 , and to a lesser extent, TbFe_2 and SmFe_2 , saturate at relatively low fields, while that of DyFe_2 is far from saturation. Since the magnetic moment is parallel to the $[111]$ crystallographic direction in TbFe_2 , SmFe_2 , ErFe_2 , and TmFe_2 , and parallel to the $[100]$ direction in DyFe_2 , this suggests that $\lambda_{111} \gg \lambda_{100}$. This is indeed the case, as we show below. The increasing magnetostriction with increasing field in the case of DyFe_2 arises from the rotation of the magnetization away from the easy $[100]$ axes, thereby sensing λ_{111} ; whereas the magnetostriction of the Tb, Er, Sm, and Tm compounds arises directly from λ_{111} . (λ_{100} and λ_{111} denote the single crystal magnetostriction constants of cubic crystals.)

In Table I, the values of the magnetostriction of some of the RFe_2 compounds are compared with those of transition metals, oxides, and other rare earth-transition metal compounds. Some of the rare earth materials are not entirely single phase and longer annealing may further increase the magnetostriction.

Single crystal magnetostriction measurements have been made to identify the source of the magnetostriction. In Figure 3, values of λ_{111} are shown for TbFe_2 and ErFe_2 . In both crystals, $[111]$ is the easy magnetization direction. Attempts to measure λ_{100} with fields up to 25 kOe proved fruitless in both cases. Although some rotation of the magnetization away from the easy $[111]$ direction occurs, no appreciable λ_{100} was detected. On the other hand, DyFe_2 and HoFe_2 possess $[100]$ easy. Here λ_{100} , rather than λ_{111} , is sensed at remanence. Surprisingly, we find the extraordinary small value

TABLE I. MAGNETOSTRICTIONS OF SOME POLYCRYSTALLINE MATERIALS AT ROOM TEMPERATURE^a

Material	$10^6 \lambda_s$	Material	$10^6 \lambda_s$
Fe	-9 ^b	YFe ₂	1.7
Ni	-35 ^b	SmFe ₂	-1560
Co	-62 ^b	TbFe ₂	1753
Sm, Tb, Dy, Ho	~ 0 ^c	TbFe ₂ (sputtered)	308
Fe ₃ O ₄	40 ^d	Tb _{.3} Dy _{.7} Fe ₂	1068
CoFe ₂ O ₄	-110 ^d	DyFe ₂	433
NiFe ₂ O ₄	-26 ^d	HoFe ₂	85 ^f
Y ₃ Fe ₅ O ₁₂	-2 ^e	ErFe ₂	-229
Tb ₂ Co ₁₇	47	TmFe ₂	-123
YCo ₃	0.4	TbFe _{1.6} Co _{.4}	1487
TbCo ₃	65	TbFe _{1.6} Ni _{.4}	1151
Tb ₂ Ni ₁₇	-4	85% Tb - 15% Fe	539
		70% Tb - 30% Fe	1590
		TbFe ₃	693
		Tb ₂ Fe ₁₇	131

- a. For the rare earth compounds, λ_s denotes $\frac{2}{3} (\lambda_{||} - \lambda_{\perp})$ at 25 kOe.
- b. See R. M. Bozorth, Ferromagnetism (Van Nostrand, New York, 1951).
- c. Non-magnetic at room temperature.
- d. See J. Smit and H. P. Wijn, Ferrites, (Wiley, New York, 1959).
- e. A. Clark, R. DeSavage, W. Coleman, E. Callen and H. Callen, J. Appl. Phys. 34, 1296 (1936).
- f. N. Koon, A. Schindler, C. Williams and F. Carter, J. Appl. Phys. 45, 5389 (1974).

of $\lambda_{100} = 4 \times 10^{-6}$ for DyFe_2 at room temperature.¹² This highly anisotropic magnetostriction establishes the importance of grain orientation. A poorly oriented polycrystal yields $\lambda_s \approx 0$; an isotropic polycrystal, $\lambda_s = .6\lambda_{111}$; and an oriented polycrystal, $\lambda_s = \lambda_{111}$. The importance of grain orientation cannot be underestimated. The effect is two-fold beneficial. As well as the obvious increase in magnetostriction, an oriented polycrystal will exhibit far lower internal losses at grain boundaries. For a good transducer material, one needs: (1) easy domain wall motion, and (2) low internal stresses at grain boundaries. The first can be achieved by sufficiently high material purity and low magnetic anisotropy, and the second by preferential grain orientation.

An atomic model of magnetostriction, based upon the high symmetry of the rare earth site in the Laves phase C15 structure, is described in reference 12. On the basis of this model, an internal distortion is coupled to the external $[111]$ strain, yielding a very large λ_{111} . On the other hand, the high $\bar{4}3m$ symmetry at the rare earth site shorts out the potentially huge λ_{100} .

There are a total of fifteen Lanthanide rare earths. In the following we point out the ones which are suitable for magnetostrictive transduction. In Table II are listed the rare earth elements in order of the increasing number of 4f electrons: Ce with one 4f electron, etc. (La with no 4f electrons and Lu with a full shell of fourteen 4f electrons are omitted.) It is possible to calculate the intrinsic ($T = 0^\circ \text{K}$) magnetostriction of each 3^+ rare earth ion for a particular compound (assuming its existence) given the magnetostriction of at least one compound (e.g., Tb^{3+} in TbFe_2). The theory utilizes the Stevens' Equivalent Operator Method. Using the measured room temperature magnetostriction of TbFe_2 and assuming single-ion temperature dependence⁸, we calculated an intrinsic value of 4400×10^{-6} for TbFe .¹⁴ According to Stevens,
14. A. Clark, J. Cullen, K. Sato, 20th Conf. on Mag. and Mag. Mat'ls, San Francisco, Calif., Dec. 1974. See AIP Conf Proc. 24, 670 (1975). See also AIP Conf. Proc. 18, 1015 (1973);

TABLE II. MAGNETOSTRICTION OF RFe₂ COMPOUNDS

R	$\alpha \times 10^2$ ^a	J	$\langle r_f^2 \rangle$ ^b	$\lambda_{111} \times 10^6$ (calc) 0°K	$\lambda_{111} \times 10^6$ (exp) room temperature
Ce	-5.72	5/2	1.20	6000	----
Pr	-2.10	4	1.086	5600	----
Nd	-0.643	9/2	1.001	2000	----
Pm	0.772	4	.942	-1800	----
Sm	4.13	5/2	.883	-3200	-2100 ^d
Eu	0	0	.834	0	----
Gd	0	7/2	.785	0	----
Tb	-1.01	6	.756	4400	2460 ^c
Dy	-0.635	15/2	.725	4200	1260 ^d
Ho	-0.222	8	.696	1600	185 ^e
Er	0.254	15/2	.666	-1500	-300 ^c
Tm	1.01	6	.639	-3700	----
Yb	3.18	7/2	.613	-3600	----

- a. K. W. H. Stevens, Proc. Phys. Soc. 65, 209 (1952)
 b. A. Freeman and R. Watson, Phys. Rev. 127, 2058 (1962)
 c. A. Clark, J. Cullen and K. Sato, AIP Conf. Proc. 24, 670 (1975)
 d. A. Clark, J. Cullen, O. McMasters and E. Callen, AIP Conf. Proc. No. 29 (1976)
 e. N. Koon, private communication

the intrinsic magnetostriction of one rare earth ion to another is given by the ratio of $\alpha J (J-1/2) \langle r_f^2 \rangle$ where α is the lowest order Stevens' factor, J is the ground state angular momentum for the 3^+ ion and $\langle r_f^2 \rangle$ is the average radius squared of the 4f electron shell. In Table II, the values of J , α , and $\langle r_f^2 \rangle$ are given along with the calculated values of λ_{111} for RFe_2 compounds. Note that the largest positive magnetoelastic interactions belong to $CeFe_2$, $PrFe_2$, $TbFe_2$ and $DyFe_2$; the largest negative interactions occur in $SmFe_2$, $TmFe_2$, and $YbFe_2$. No magnetostriction is predicted for $GdFe_2$ and $EuFe_2$ on the basis of this model. The elements Ce and Yb are not useful magnetostrictively since Ce is found in its quadrivalent state, Ce^{4+} , and Yb in its divalent state, Yb^{2+} , yielding zero magnetostriction. $PmFe_2$ is radioactive, and $PrFe_2$ and $NdFe_2$ do not readily form the cubic Laves phase compounds. This leaves $TbFe_2$ and $DyFe_2$ as the two most promising candidates for high room temperature (positive) magnetostriction. Dy is eliminated for practical reasons because $[100]$ is the easy magnetization direction and $\lambda_{100} \ll \lambda_{111}$. See Section III. For negative magnetostriction, $TmFe_2$ and $SmFe_2$ are most promising. $SmFe_2$ emerges because of its high Curie temperature and much lower cost.

Values of λ_{111} at room temperature depend upon the intrinsic magnetostriction plus the rare earth sublattice magnetization at this temperature. The higher the Curie temperature the higher the sublattice magnetization and the higher the magnetostriction. Room temperature experimental values for λ_{111} are given in the table for $SmFe_2$, $TbFe_2$, $HoFe_2$ and $ErFe_2$.

As pointed out earlier, the saturation values of magnetostriction for a polycrystal, λ_s , depend upon the degree of orientation of crystallites. For isotropic crystallite distribution, $\lambda_s = (2\lambda_{100} + 3\lambda_{111})/5$; and since $\lambda_{100} \ll \lambda_{111}$, it follows that

$\lambda_s \cong .6 \lambda_{111}$. For preferential orientation, $.6\lambda_{111} < \lambda_s < \lambda_{111}$. The values of λ_{111} in Table II can be compared to the values for polycrystals in Figure 2 and Table I.

III. MAGNETIC ANISOTROPY

Magnetic anisotropy refers to the difference in energy required to rotate the magnetization from one crystalline direction to another. This energy is often expressed in direction cosines (α_j 's) of the magnetization with respect to the crystalline axes. For cubic crystals the lowest order expression is:

$$K = K_1(\alpha_1^2\alpha_2^2 + \alpha_2^2\alpha_3^2 + \alpha_3^2\alpha_1^2).$$

If $K_1 < 0$; the energy is lowest when the magnetization points along the [111] direction; if $K_1 > 0$, [100] is the preferred direction of magnetization. When [111] is easy, λ_{111} is sensed at remanence; when [100] is easy, λ_{100} is sensed. The total expression for the anisotropy is in general an infinite series. As higher order terms are taken into account, other directions may become easy and the magnetostriction referred to that direction is sensed. In some cases, e.g., some ternary alloys, the easy direction is a function of temperature.¹⁵

Magnetic anisotropy values were determined both by magnetization measurements and magnetic torque measurements.^{16,17} Both methods employ single crystals. Using the former method, the anisotropy can be calculated from magnetization measurements along various

15. U. Atzmony, M. P. Dariel, E. R. Bauminger, D. Lebenbaum, I. Nowik and S. Ofer, Phys. Rev. B7, 4220 (1973)
16. A. Clark, H. Belson, and N. Tamagawa, Phys. Letters 42A, 160 (1972); also AIP Conf. Proc. 10, 749 (1973)
17. C. Williams, N. Koon, and J. Milstein, 21st Conf. on Mag. and Mag. Mat'ls Philadelphia, Pa., Dec. 1975; AIP Conf. Proc. No. 29 (1976).

crystallographic directions. This method is useful when the anisotropy is very large. Torque methods are more accurate and are particularly useful for moderate and low magnetic anisotropies. The largest recorded anisotropy of a cubic crystal at room temperature is that of TbFe_2 .¹⁴ It is negative. The largest known positive anisotropy is that of DyFe_2 .¹⁶ In Figure 4 we illustrate the magnetization curves for TbFe_2 at room temperature along the three principal crystallographic directions in fields up to 120 kOe.¹⁸ Note that even at this huge field, the moment cannot be aligned along its hard [100] direction. The anisotropy energy is too high. Similar curves exist for DyFe_2 . For ErFe_2 , the anisotropy at room temperature is smaller because of its lower Curie temperature. However, it becomes enormous at low temperatures. In Figure 5, we show the magnetization curves vs. H for ErFe_2 at 4°K. From these measurements, we estimate $K_1(4^\circ\text{K}) \approx -5 \times 10^8 \text{ erg/cm}^3$, the largest known cubic magnetic anisotropy. Comparable magnitudes are calculated for anisotropies of TbFe_2 and DyFe_2 at this temperature.

In Table III we list the anisotropy constants of some cubic metals and ferrites at room temperature. Here the large difference between the anisotropies of the RFe_2 compounds and the cubic transition metal alloys is clearly shown. In the next section we describe a method to reduce the magnetic anisotropy.

IV. MAGNETOSTRICTION OF PSEUDO-BINARY LAVES PHASE COMPOUNDS

For many magnetostrictive transducer applications, the figure of merit contains the ratio of the square of the magnetostriction to the anisotropy energy.⁴ One therefore looks for materials with small anisotropy energy, as well as with large magnetostriction. In Table IV are the signs of λ , K_1 and K_2 for the RFe_2 compounds, taken from our measurements and from theoretical estimates. K_1

18. Magnetic fields were obtained at the NRL High Field Facility, Washington, D. C.

TABLE III. ANISOTROPY CONSTANTS OF SOME CUBIC METALS
AND FERRITES AT ROOM TEMPERATURE

Metal	$10^{-4}K_1$ (ergs/cm ³)	Ferrite	$10^{-4}K_1$ (ergs/cm ³)
Fe	45 ^a		
Ni	-5 ^a		
70% Fe-Co	-43 ^b		
65% Co-Ni	-26 ^c		
ErFe ₂	-330	Ga _{.44} Fe _{2.54} O ₄	-81 ^d
DyFe ₂	2100	CoFe ₂ O ₄	260 ^e
TbFe ₂	-7600	Co _{.8} Fe _{2.2} O ₄	290 ^f
HoFe ₂	360 ^g	Co _{.3} Zn _{.2} Fe _{2.2} O ₄	150 ^f

- a. U. Hoffman, Z. angew. Phys. 22, 106 (1967).
 b. L. W. McKeenan, Phys. Rev. 51, 136 (1937).
 c. J. W. Shih, Phys. Rev. 50, 376 (1936).
 d. R. F. Pearson, J. Appl. Phys. 31, 160S (1960).
 e. R. Perthel, G. Elbinger, and W. Keileg, Phys. Status Solidi
 17, 151 (1966).
 f. F. M. Bozorth, E. R. Tilden, and A. J. Williams, Phys. Rev. 99,
 1788 (1955).
 g. C. Williams, N. Koon and J. Milstein, Proc. 21st Conf. on Mag.
 & Mag. Mat'ls., Philadelphia, Pa., Dec. 1975.

TABLE IV. POLARITY OF λ , K_1 and K_2

	PrFe_2	SmFe_2	TbFe_2	DyFe_2	HoFe_2	ErFe_2	TmFe_2	YbFe_2
λ	+	-	+	+	+	-	-	-
K_1	+	-	-	+	+	-	-	+
K_2	-	0	+	-	+	-	+	-

and K_2 are the coefficients of the two lowest terms in the magnetic anisotropy expression for cubic materials.

Using this table, we can construct pseudobinary compounds in such a way as to minimize the magnetic anisotropy while maintaining a large positive (or negative) magnetostriction. The procedure is to select compounds with the same magnetostriction sign (if possible) but with opposite signs of anisotropy. Attractive ternary compounds yielding a positive magnetostriction are $Tb_{1-x}Dy_xFe_2$ (Terfenol-D), $Tb_{1-x}Ho_xFe_2$, and $Tb_{1-x}Pr_xFe_2$ (Terfenol-P). The compounds of negative magnetostriction are $Sm_{1-x}Ho_xFe_2$ (Samfenol-H), $Sm_{1-x}Dy_xFe_2$, (Samfenol-D), and $Sm_{1-x}Yb_xFe_2$. In each case x can be chosen to maximize λ^2/K_{tot} .

The largest saturation magnetostrictions have been found in the Terfenol-D and Terfenol-P systems. The Terfenol-D system has been investigated in detail. In Figure 6 we plot the magnetostriction of polycrystalline arc-cast and annealed samples of $Tb_{1-x}Dy_xFe_2$ for $H = 10$ kOe and $H = 25$ kOe. Near $x = .7$, the magnetostriction at these fields exhibit a peak reflecting the near zero magnetic anisotropy at this concentration. In Figure 7 we illustrate how the value of the saturation magnetostriction constant λ_{111} varies with Dy concentration. λ_{111} was determined by X-Ray techniques, utilizing a method developed to accurately pinpoint the value of x for anisotropy sign reversal.¹² It was shown that the magnetostrictive properties of this alloy system degrade rapidly as x becomes greater than .75. This is reflected in the rapid drop of the magnetomechanical coupling factor k_{33} shown below. See reference 19.

x	.5	.7	.74	.76	.8
k_{33}	.48	.53	.6	.4	.23

19. H. Savage, A. Clark, and J. Powers, IEEE Trans. on Mag. MAG-11, 1355 (1975)

UNCLASSIFIED
NSWC/WOL/TR 76-99

$Tb_{.27}Dy_{.73}Fe_{1.95}$ is the material presently used in the prototype transduction devices developed at USRD/NRL, NUC, Raytheon, and Honeywell. Some of the properties are gathered below:

- | | |
|---|--|
| a. Saturation Magnetostriction | $\lambda_s = 1000 \text{ to } 1100 \times 10^{-6}$ |
| b. $d\lambda/dH$ | $d = 8 \text{ to } 10 \times 10^{-9} \text{ m/a}$ |
| c. Magnetization | $M = .98 \text{ Tesla}$ |
| d. Density | $\rho = 9.2 \text{ g/cm}^3$ |
| e. Resistivity ($TbFe_2$) | $\rho = 60 \mu\Omega\text{cm}$ |
| f. Sound velocity (200 Oe) | $v = 2300 \text{ m/sec}$ |
| g. Young's Modulus (200 Oe) | $E = 5 \times 10^{10} \text{ newton/m}^2$ |
| h. Magnetomechanical Coupling
(200 Oe) | $k_{33} = .52 \text{ to } .6$ |
| i. Permeability (200 Oe) | $\mu_r = 4$ |

The magnetostrictive properties of a new alloy, $Tb_{1-x}Pr_xFe_2$, are currently being investigated. Pr has a huge intrinsic magnetostriction and is far less expensive than Tb. However, it does not crystallize in the cubic $PrFe_2$ structure. In Figure 8 we show magnetostriction vs. H for some $Tb_{1-x}Pr_xFe_2$ alloys. Initial results indicate that only 20% to 30% $PrFe_2$ can be added to $TbFe_2$ before 2nd phase material appears. The highest measured constant, $d\lambda/dH$, occurs for $Tb_{.9}Pr_{.1}Fe_2$. X-Ray determination of λ_{111} indicates an almost constant value of λ_{111} for $1 > x > .7$. See Figure 9.

Positive magnetostriction pseudobinary compounds containing three rare earths have also been examined. Two important systems under consideration are $Pr_xTb_yDy_zFe_2$ and $Tb_xDy_yHo_zFe_2$ ($x + y + z = 1$). In both systems, the two lowest order anisotropy constants can be simultaneously minimized, if necessary. Values of λ_{111} for some compounds are shown in Table V. The uncertainty is $\pm 100 \times 10^{-6}$. All compounds have [111] easy.

It is more difficult to find a good pseudobinary compound to achieve a large λ^2/K for negative magnetostriction. Yb, an important

TABLE V. MAGNETOSTRICTION OF QUATERNARY COMPOUNDS

Compound	$\lambda_{111} \times 10^6$	Compound	$\lambda_{111} \times 10^6$
Tb _{.3} Pr _{.1} Dy _{.6} Fe ₂	1750	Tb _{.26} Dy _{.53} Ho _{.21} Fe ₂	1460
Tb _{.3} Pr _{.2} Dy _{.5} Fe ₂	1760	Tb _{.23} Dy _{.35} Ho _{.42} Fe ₂	1135
		Tb _{.19} Dy _{.18} Ho _{.63} Fe ₂	810

component, is not found in the trivalent state. However, compounds can be selected which compensate anisotropy and magnetostriction, however, at different values of x . Two important pseudobinaries are $\text{Sm}_{1-x}\text{Dy}_x\text{Fe}_2$ and $\text{Sm}_{1-x}\text{Ho}_x\text{Fe}_2$. Unfortunately, here both λ and K_1 have opposite signs. However, the anisotropy is compensated with small additions of Dy and Ho, yielding a magnetostriction $|\lambda|$ at compensation which is greater than 1000×10^{-6} . In Figure 9 we show values of λ_{111} for $\text{Sm}_{1-x}\text{Ho}_x\text{Fe}_2$ and $\text{Sm}_{1-x}\text{Dy}_x\text{Fe}_2$. For $\text{Sm}_{1-x}\text{Ho}_x\text{Fe}_2$, compensation occurs near $x = .3$; for $\text{Sm}_{1-x}\text{Dy}_x\text{Fe}_2$, compensation occurs near $x = .15$.

In view of this, we propose a bender bar (or magnetostriction multiplier) configuration composed of $\text{Tb}_{.27}\text{Dy}_{.73}\text{Fe}_2$ ($\lambda > 1000 \times 10^{-6}$) vs. $\text{Sm}_{.15}\text{Dy}_{.85}\text{Fe}_2$ ($\lambda < 1000 \times 10^{-6}$).

V. ELASTIC ENERGIES AND THE ΔE EFFECT

Room temperature sound velocities, densities, and moduli are listed in Table VI for TbFe_2 , ErFe_2 , YFe_2 and TbFe_3 .²⁰ Longitudinal and shear velocities were measured ultrasonically at 7 MHz. The moduli are midway between those of the soft rare earth elements and the stiffer magnetic transition metals, such as Fe and Ni.

The moderate magnitudes of the moduli and the huge magnitudes of the magnetostrictions combine to yield huge magnetoelastic forces and energies for these compounds. Values for λ_s , $E\lambda_s$, and the energy density, $\frac{1}{2}E\lambda_s^2$, are shown in Table VI. They are compared to those of elemental Ni, a typical magnetostrictive material. The quantity $E\lambda_s$ is a measure of the force exerted by a constrained bar of the material which is magnetized to saturation. The energy density, $\frac{1}{2}E\lambda_s^2$, represents the amount of magnetic energy which can be transformed to elastic energy per unit volume of the material. For TbFe_2 , this energy is about 1000 times that of earlier magnetostrictive materials, such as Ni.

20. A. Clark, H. Belson, and R. Strakna, J. Appl. Phys. 44, 2913 (1973)

TABLE VI. ELASTIC AND MAGNETOELASTIC PROPERTIES

	TbFe ₂	ErFe ₂	YFe ₂	TbFe ₃	Ni
v _l (m/sec)	3940	4120	4340	4230	---
v _s (m/sec)	1980	2180	2720	2340	---
ρ (gm/cm ³)	9.0	9.7	6.7	9.4	---
E x 10 ⁻¹⁰ (newton/m ²)	9.4	12.1	12.7	13.1	21 ^a
λ _s x 10 ⁶	1750	-229	--	693	-33 ^b
Eλ _s x 10 ⁻⁷ (newton/m ²)	17	2.8	--	9	.7
Eλ _s ² /2 x 10 ⁻³ (joule/m ³)	145	3.2	--	32	.1

a. "Nickel," The International Nickel Co., Inc., 1951.

b. J. J. Went, Physica 17, 98 (1951).

Closely related to the magnetostriction is the " ΔE Effect", i.e., the fractional change in Young's modulus between the magnetically saturated state and the unmagnetized state. Because of the huge magnetostrictive effects in the RFe_2 compounds, a large " ΔE Effect" at room temperature occurs.²¹ We observed the change in resonant frequency at constant current as a function of magnetic field in a thin bar of $Tb_{.3}Dy_{.7}Fe_2$ resonating near 15 kHz. From this, we calculated the corresponding sound velocity and modulus. The dependence of Young's modulus on magnetic field is shown in Figure 10. We find that the modulus increases by about 150%. This increase is by far the largest known and reflects a sound velocity change of $\sim 60\%$ upon magnetic saturation.²¹ Thus, RFe_2 magnetostrictive compounds have unusual potential as adjustable frequency resonators, filters, and acoustic delay lines, as well as for high power energy converting devices.

More Detailed compliance and magnetomechanical coupling measurements are reported in reference 19.

VI. RESISTIVITY AND MAGNETORESISTANCE OF $TbFe_2$

The electrical resistivity is an important parameter for many applications. In Figure 11, we show the electrical resistivity of $TbFe_2$ as measured by Savage.²² The transverse magnetoresistivity at room temperature is almost linear in fields to 10 kOe, yielding $\Delta\rho/\rho H = 7.5 \times 10^{-9}$ m/a.

VII. FABRICATION OF TRANSDUCER ELEMENTS

Further improved magnetic and magnetostrictive properties depend upon grain orientation. This is convincingly shown by $\lambda_{111} \gg \lambda_{100}$.

21. A. Clark and H. Savage, IEEE Trans. on Sonics and Ultrasonics SU-22, 50 (1975)
22. H. Savage, Naval Surface Weapons Center, White Oak, Silver Spring, Md. 20910

Grain orientation has two profound effects: (1) increased saturation magnetostriction, λ_s , and (2) decreased internal strains at grain boundaries. The benefit of the first effect is obvious. Complete grain alignment would achieve an increase in λ_s of $\sim 50\%$. The second effect is perhaps far more significant. Presently the biggest obstacle to higher permeability and coupling factor are the large internal strains commonly developed at grain boundaries in highly magnetostrictive materials. These internal strains depend upon the state of magnetization. During the process of magnetization internal energies are developed which produce no useful external work. The overall effect is to degrade the high intrinsic permeability and d constant.

Thus the method used to fabricate transducer elements, if possible, should be adaptable to grain orientation. The transducer alloys also should be as free as possible from imperfections such as voids, inclusion, etc., which inhibit rapid domain wall motion. Other criteria are low cost, ability to produce large sizes and various configuration, and, in some cases, the ability to laminate and construct bimetallic elements. The transducer elements should also have adequate toughness and resistance to shock.

It is unlikely that all these desirable features can be embodied in one fabrication method. Powder metallurgy has a great advantage that it is adaptable to grain orientation and grain size control. Powder metallurgy techniques, similar to those necessary here, have already been employed for permanent magnet fabrication. Presently vacuum sintering of grain oriented powders is being carried out at NSWC. Dense materials have already been prepared by vacuum hot press methods at Raytheon. Arc-Plasma Deposition, another attractive technique, has the advantage of simplicity and ease of laminating. Rings have been produced by Arc-Plasma Deposition at Union Carbide. These methods, and others, such as arc-casting, vacuum casting, epoxy encapsulation and particulate composites are presently being explored.

VIII. SUMMARY

The rare earth intermetallic compounds have opened up a new era in magnetostrictive materials. Only a few years ago magnetostrictions of 1000 to 3000 ppm were non-existent. Today we have many materials with these magnetostrictions at room temperature and above. These materials rely on two highly magnetoelastic rare earth elements: Tb and Sm, plus the element iron, which lifts the magnetostriction to room temperature. Alloys have been developed with coupling factors equivalent to those of piezoelectric ceramics ($k \cong .6$), far greater than typical magnetostrictive materials. Many static and dynamic properties of these alloys have been investigated. They include magnetostriction elastic moduli, permeability, magnetomechanical coupling, anisotropy, and resistivity. Some prototype transducers have been designed and constructed.

The rare earth alloys are not yet optimized for transducer performance. New systems are under investigation. Giant strides are expected by grain orientation and the reduction of imperfections. Substantial increases in permeability and coupling factor are forecast. Toughened samples also appear imminent.

New transduction configurations and methods of excitation are expected to emerge because of the new features of rare earth materials. An attractive possibility utilizes bimetallic strips of highly magnetostriction materials. A novel innovation is a composite transducers containing both magnetostrictive and piezoelectric materials.

Magnetostrictive materials, of course, are not limited to their use in sonar transducers. Valves, actuators, resonators, etc., are expected to employ rare earth materials. As interest in the rare earths for these applications grows, the research base will widen and ultimately yield still further improved materials.

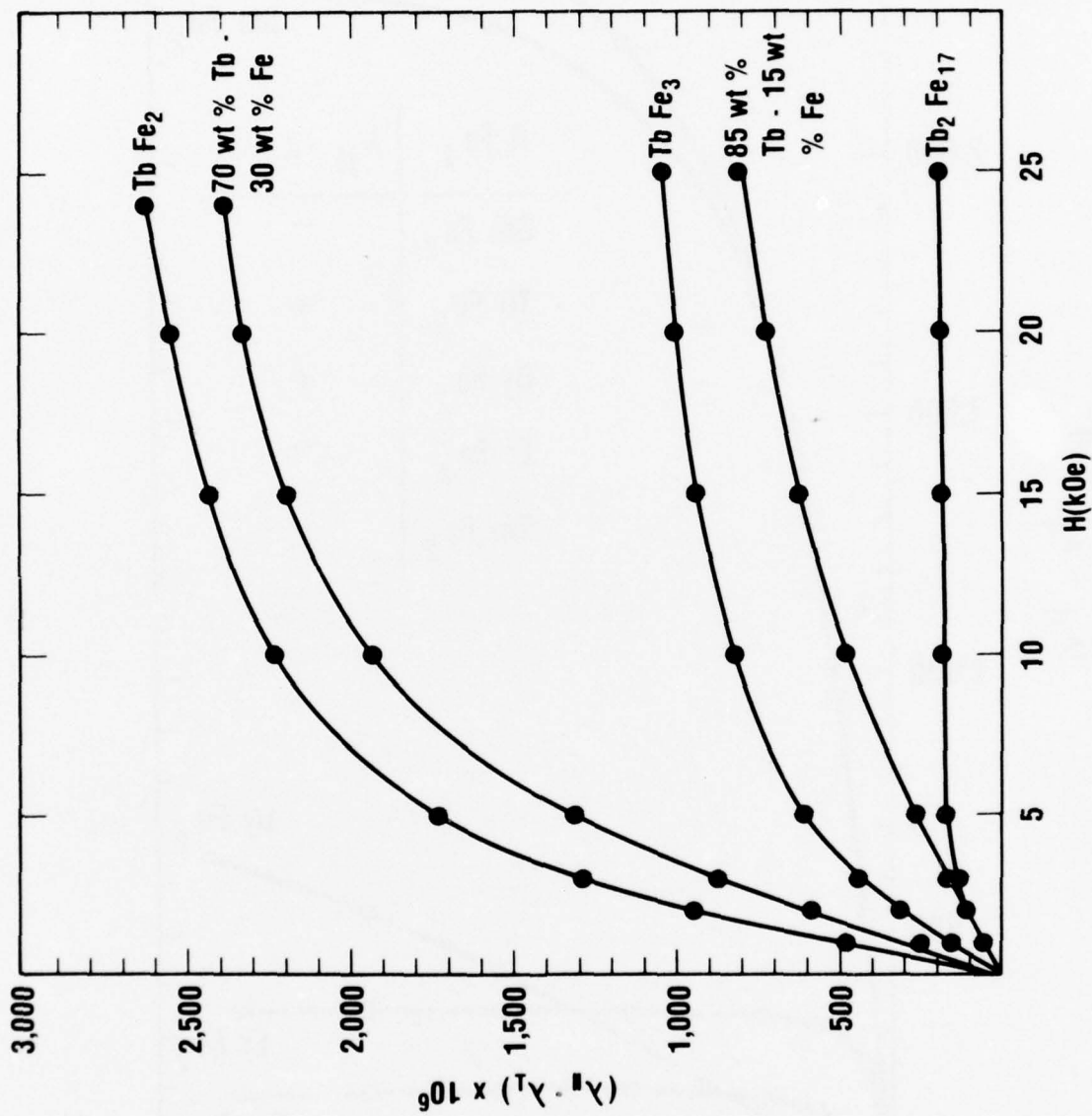


Fig. 1 Magnetostriction of Tb-Fe Alloys

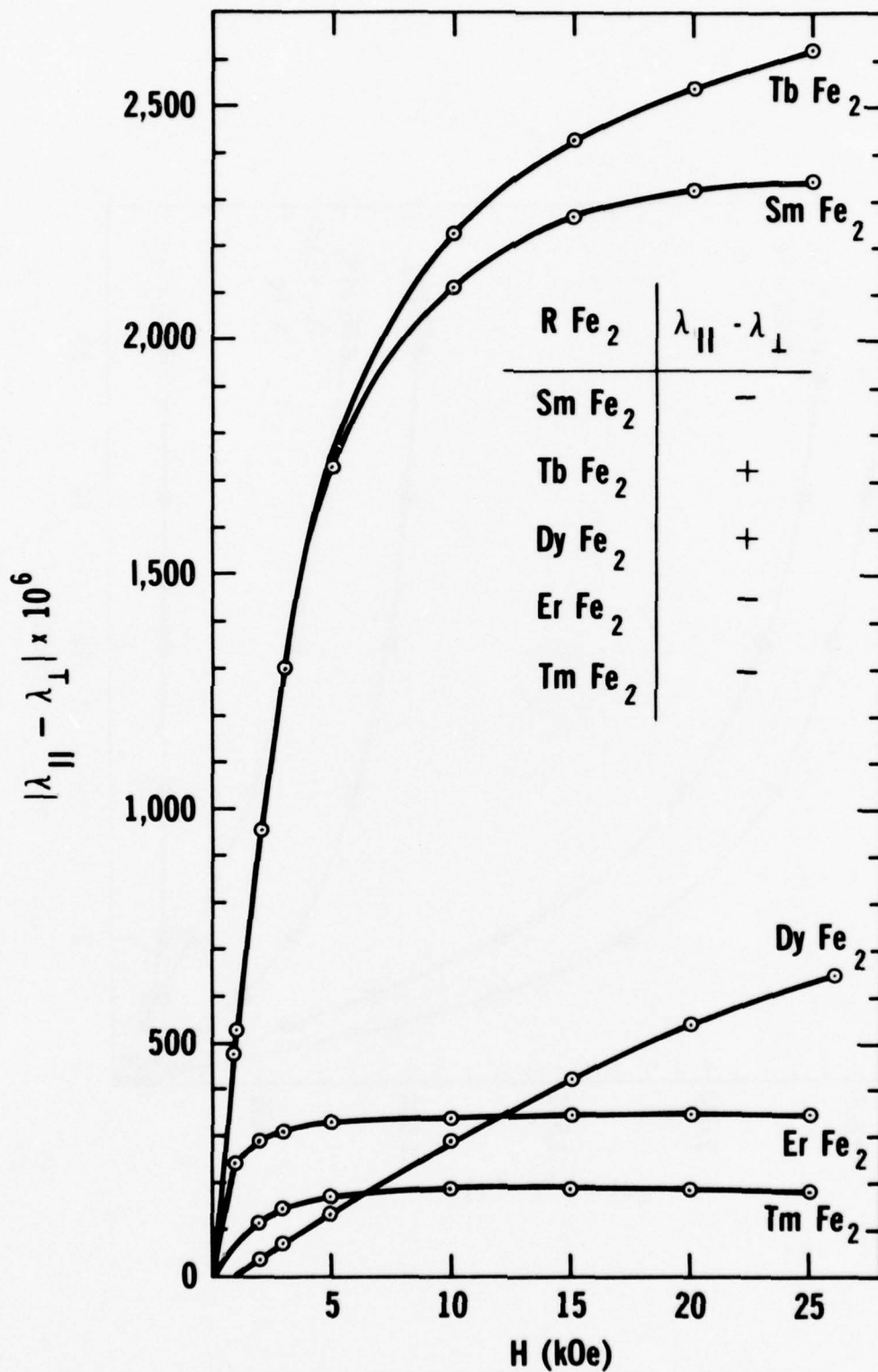


Fig. 2 Magnetostriction of RFe_2 Compounds

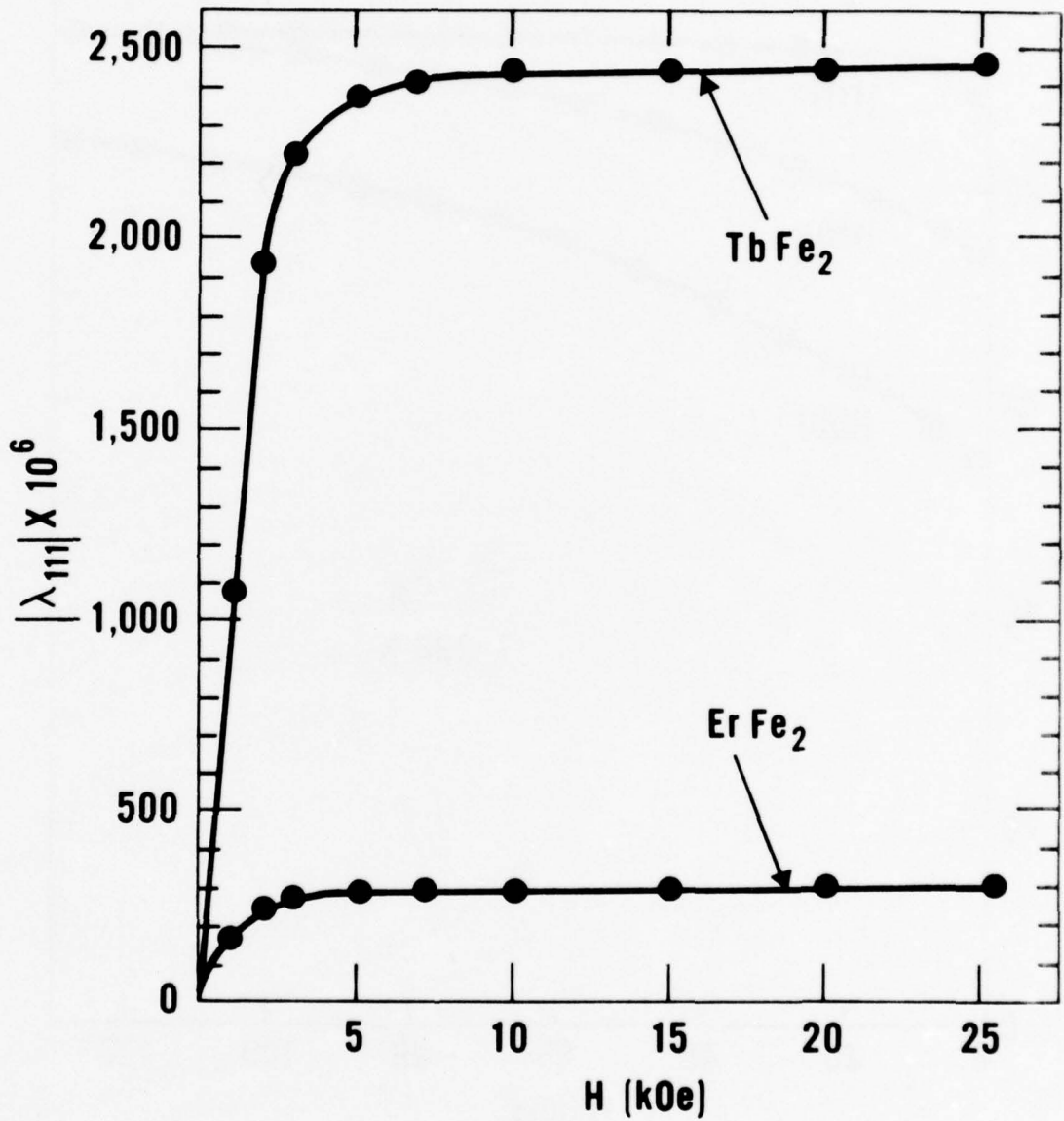


Fig. 3 Magnetostriction of Single Crystal $TbFe_2$ and $ErFe_2$. For $TbFe_2$, $\lambda_{111} > 0$; for $ErFe_2$, $\lambda_{111} < 0$.

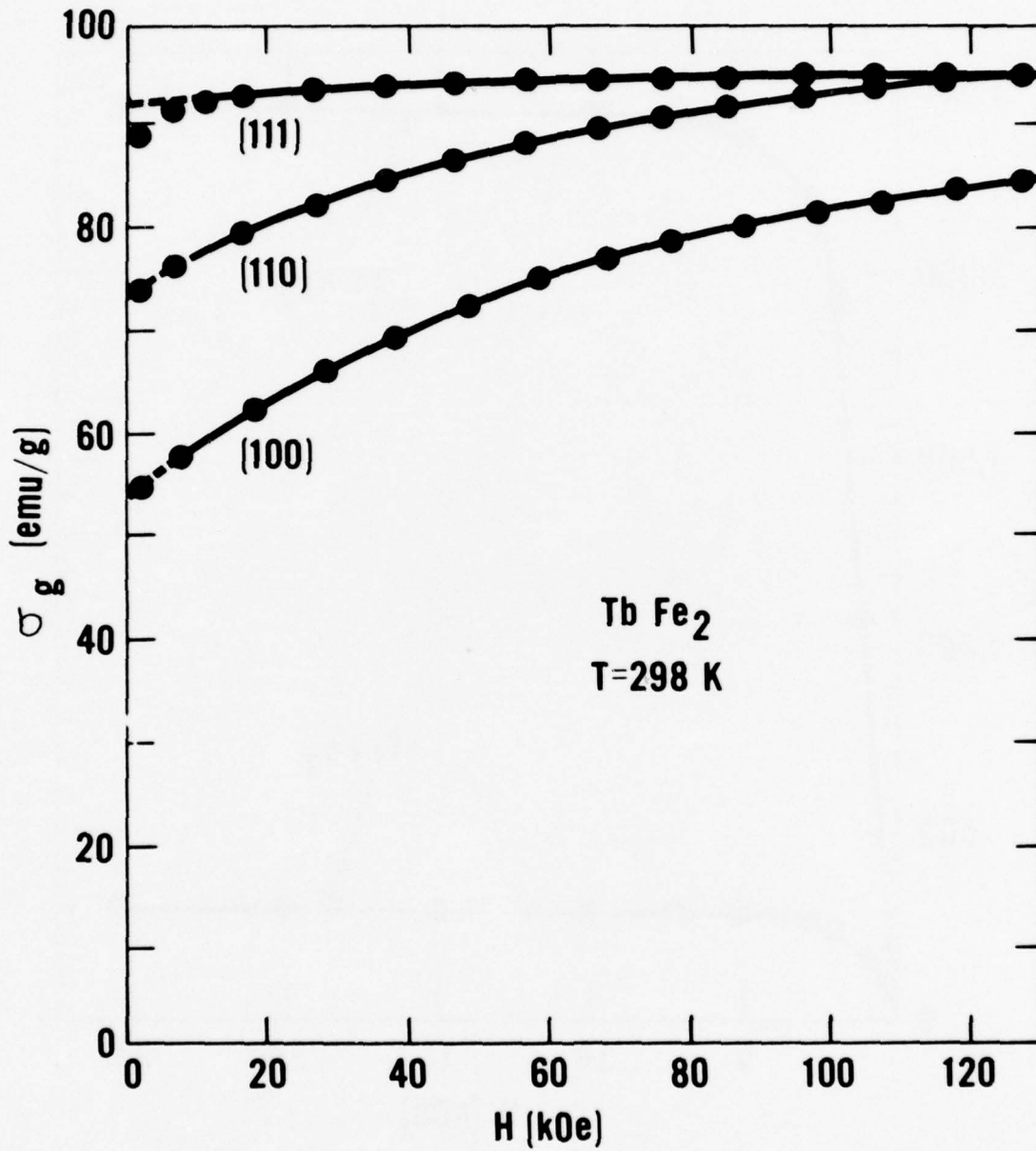


Fig. 4 Room Temperature Magnetic Moment of Single Crystal TbFe₂.

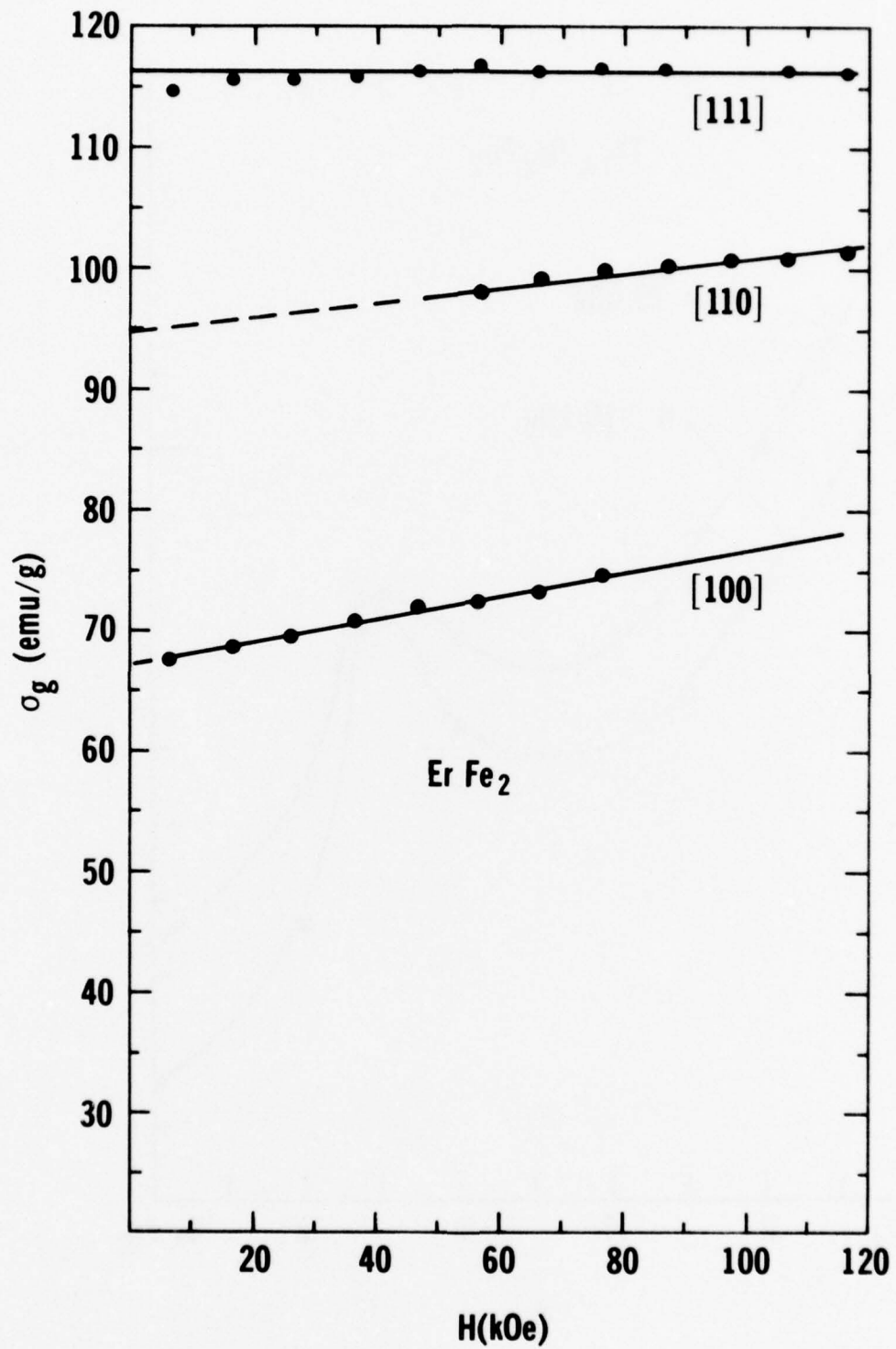


Fig. 5 Magnetic Moment of Single Crystal ErFe_2 at 4.2°K .

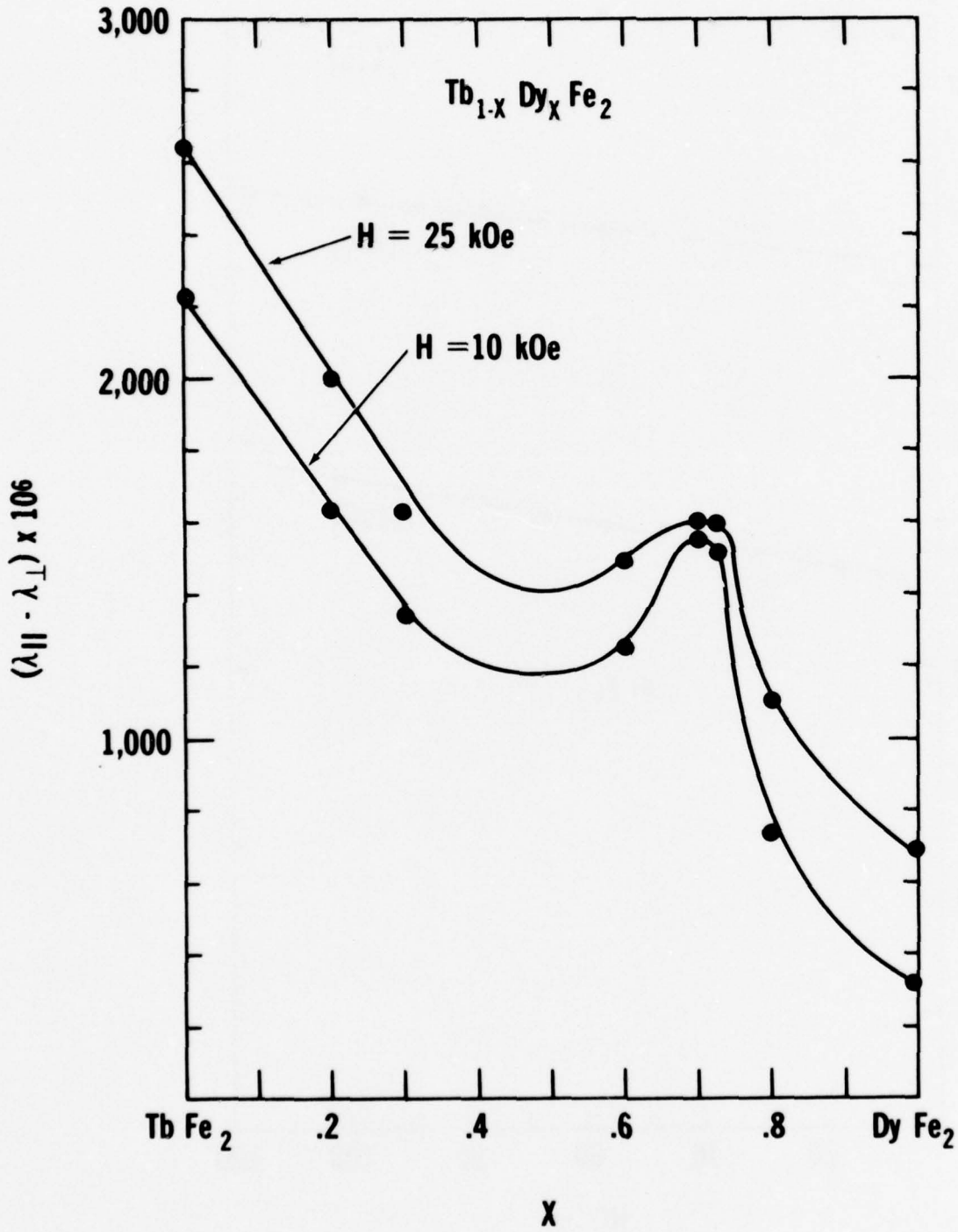


Fig. 6 Magnetostriction of $Tb_{1-x} Dy_x Fe_2$ at Fields of 10 kOe and 25 kOe.

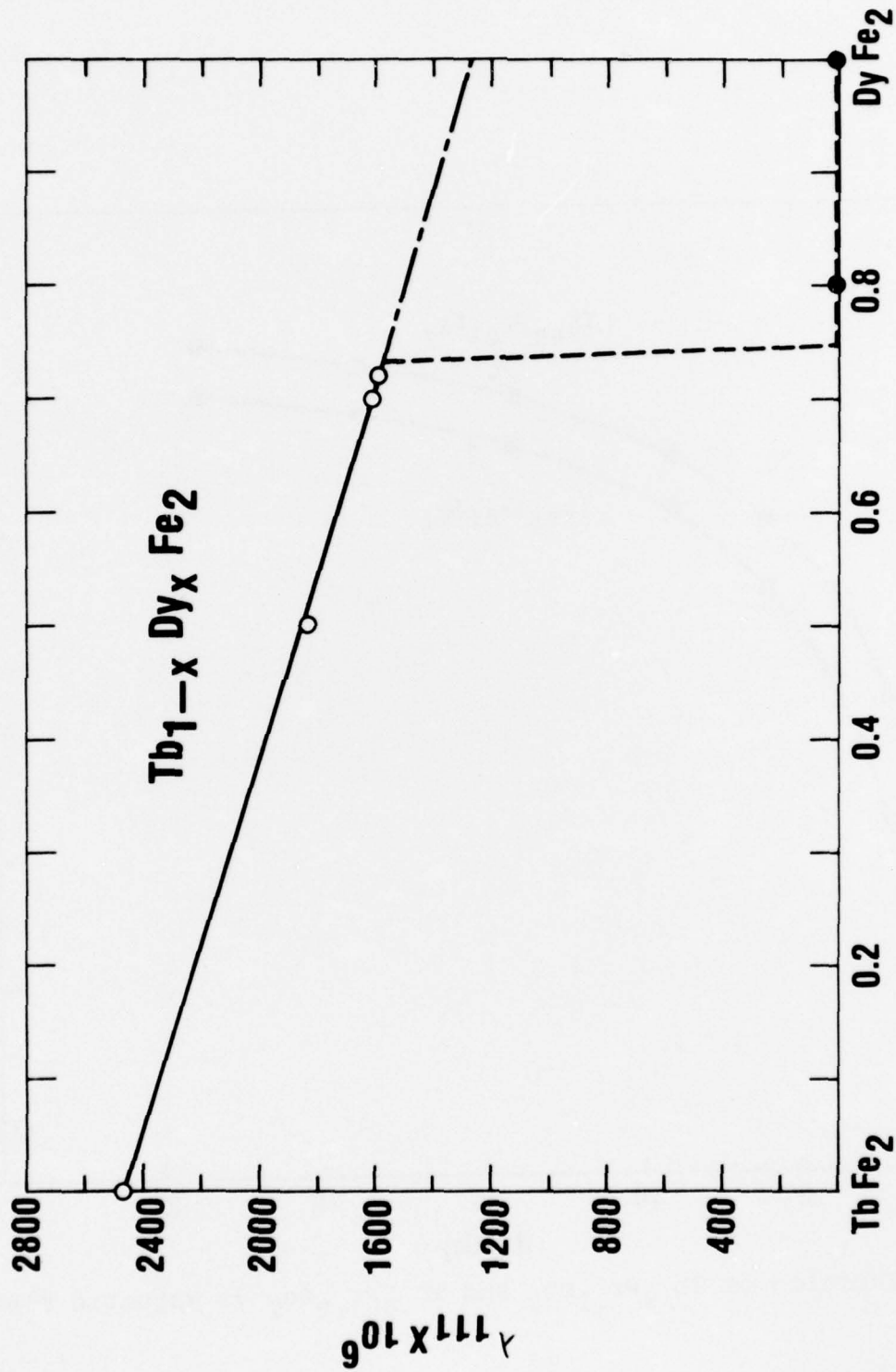


Fig. 7 Magnetostriction Constant λ_{111} determined by x-ray method

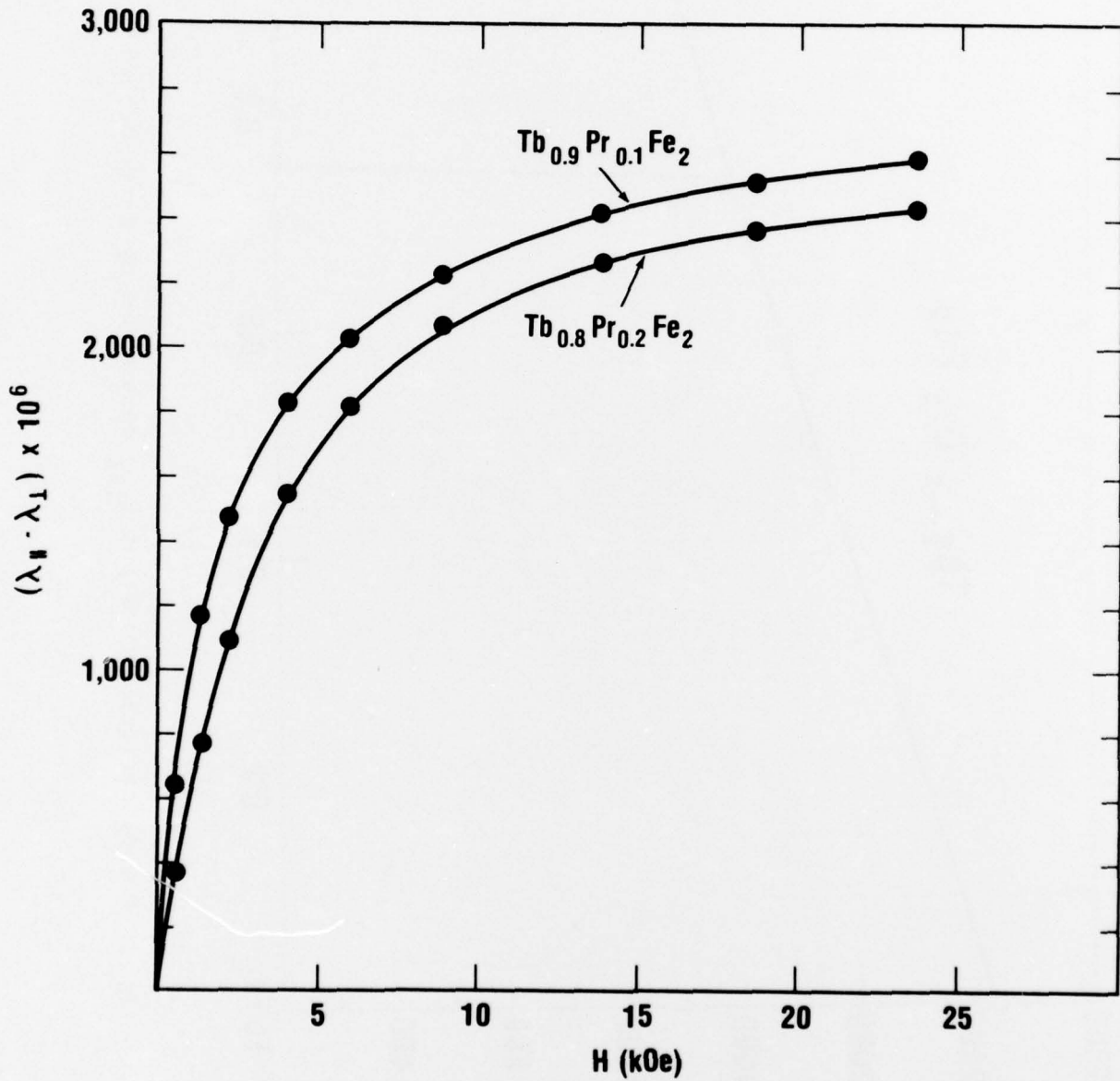


Fig. 8 Magnetostriction of $Tb_{0.9}Pr_{0.1}Fe_2$ and $Tb_{0.8}Pr_{0.2}Fe_2$ vs Magnetic Field

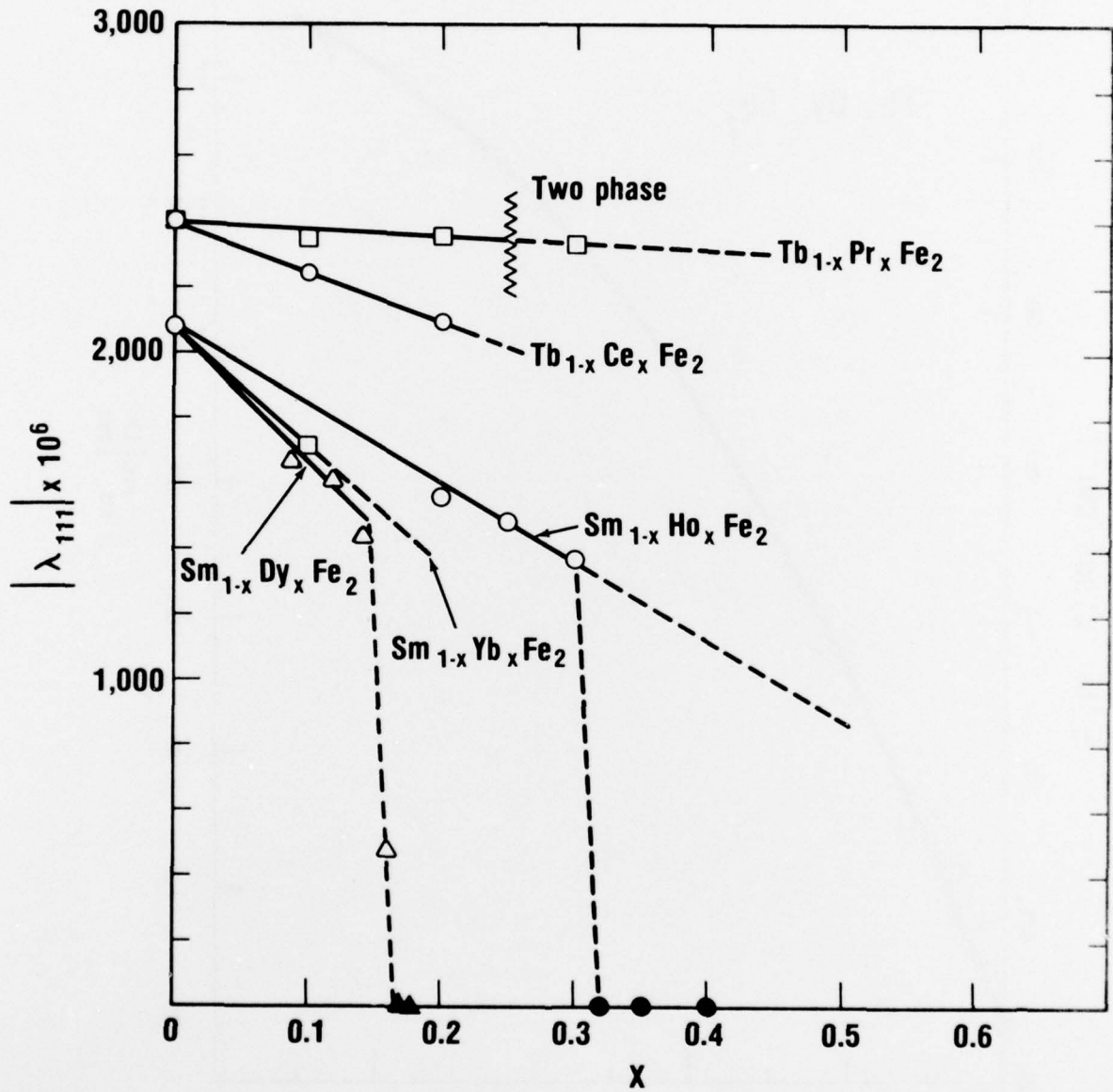


Fig. 9 Magnetostriction Constant λ_{111} for some Ternary Rare Earth - Fe_2 Compounds. For Tb Compounds, $\lambda_{111} > 0$, for Sm compounds, $\lambda_{111} < 0$.

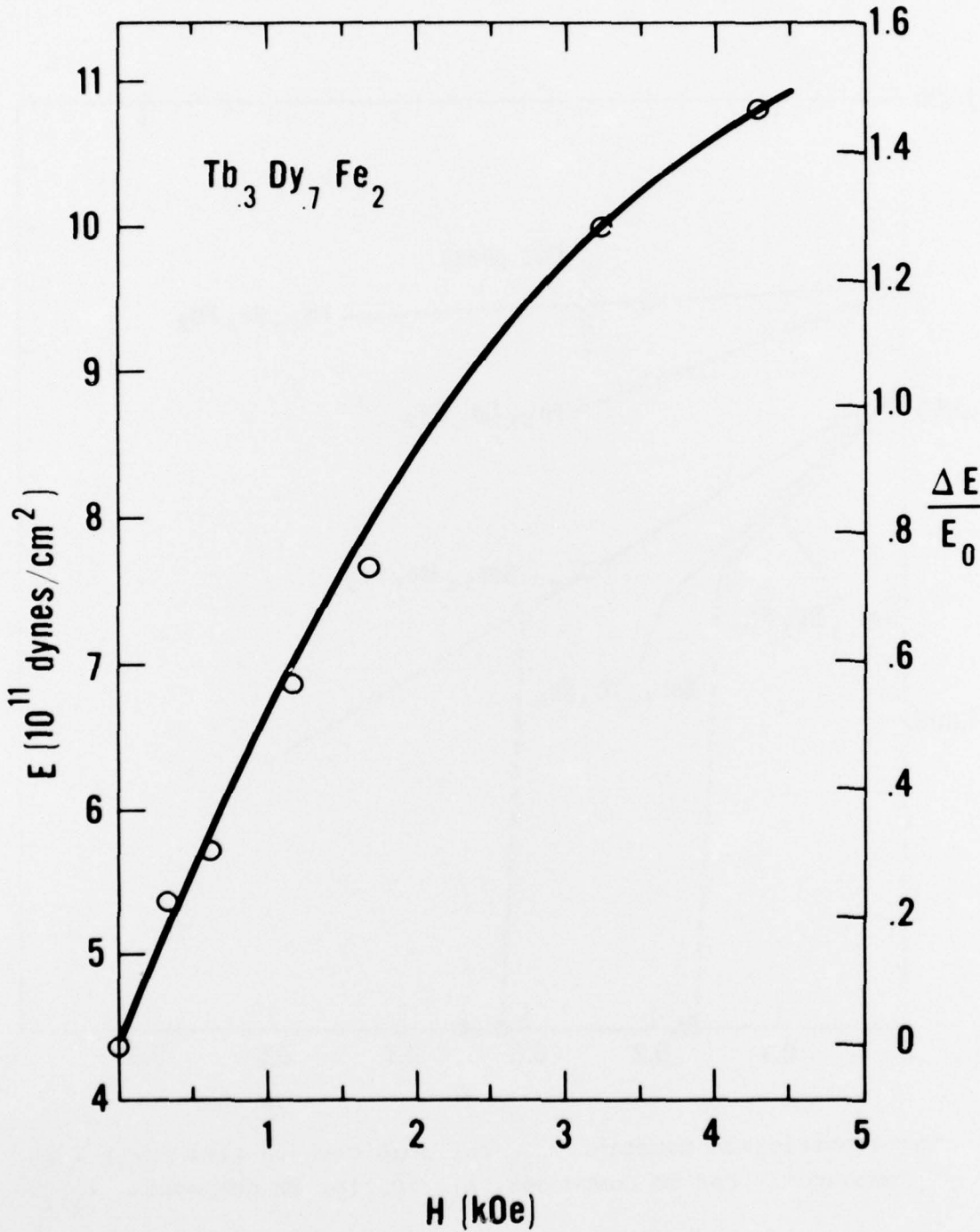


Fig. 10 Elastic Modulus and ΔE Effect in Terfenol-D.

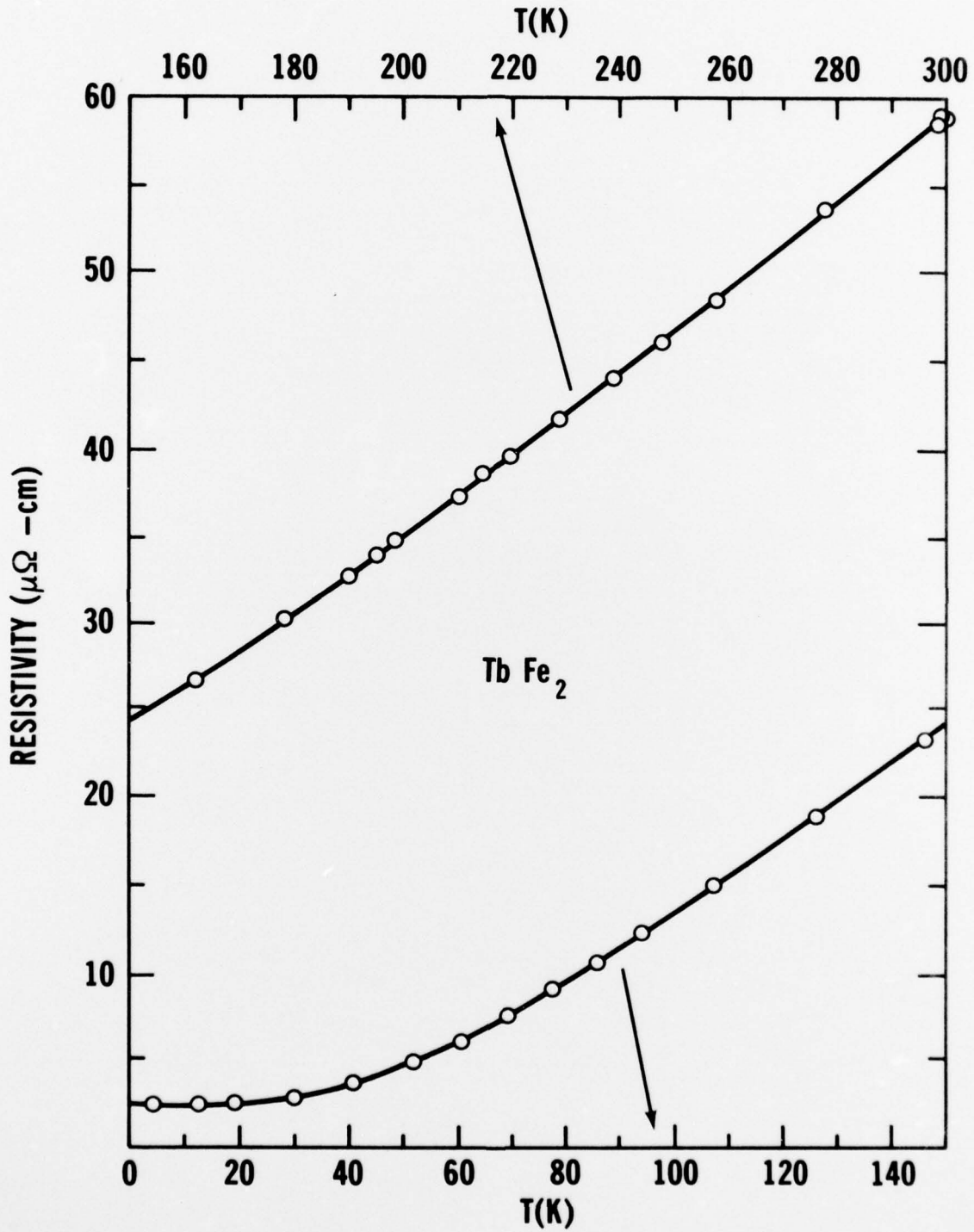


Fig. 11 Resistivity of TbFe₂.

DISTRIBUTION LIST

	Copies
Defense Documentation Center Cameron Station Alexandria, Virginia 22314	12
Office of Naval Research Arlington, Va. 22217 Attn: Code 4/1 Code 102 Code 470 Code 200	1 1 1 1
Commanding Officer Office of Naval Research Branch Office 495 Summer Street Boston, Massachusetts 02210	1
Commanding Officer Office of Naval Research Branch Office 536 South Clark Street Chicago, Illinois 60605	1
Office of Naval Research San Francisco Area Office 760 Market Street, Room 447 San Francisco, California 94102 Attn: Dr. P. A. Miller	1
Naval Research Laboratory Washington, D. C. 20390 Attn: Code 6000 Code 6100 Code 6300 Code 6400 Code 2627	1 1 1 1 1

UNCLASSIFIED
NSWC/WOL/TR 76-99

DIST. Cont.

	Copies
Naval Air Development Center Code 302 Warminster, Pennsylvania 18974 Attn: Mr. F. S. Williams	1
Naval Air Propulsion Test Center Trenton, New Jersey 08628 Attn: Library	1
Naval Construction Battalion Civil Engineering Laboratory Port Hueneme, California 93043 Attn: Materials Division	1
Naval Electronics Laboratory Center San Diego, California 92152 Attn: Electron Materials Sciences Division	1
Naval Missile Center Materials Consultant Code 3312-1 Point Mugu, California 93041	1
	1
David W. Taylor Naval Ship R&D Center Materials Department Annapolis, Maryland 21402	1
Naval Undersea Center San Diego, California 92132 Attn: Library	1
Naval Underwater System Center Newport, Rhode Island 02840 Attn: Library	1
Naval Weapons Center China Lake, California 93555 Attn: Library	1

UNCLASSIFIED
NSWC/WOL/TR 76-99

DIST. Cont.

	Copies
Naval Postgraduate School Monterey, California 93940 Attn: Mechanical Engineering Department	1
Naval Air Systems Command Washington, D. C. 20360 Attn: Code 52031	1
Code 52032	1
Code 320	1
Naval Sea Systems Command Washington, D. C. 20362 Attn: Code 035	1
SEA-03B	1
Naval Facilities Engineering Command Alexandria, Virginia 22331 Attn: Code 03	1
Scientific Advisor Commandant of the Marine Corps Washington, D. C. 20380 Attn: Code AX	1
Naval Ship Engineering Center Department of the Navy CTR BG #2 3700 East-West Highway Prince Georges Plaza Hyattsville, Maryland 20782 Attn: Engineering Materials and Services Office, Code 6101	1
Army Research Office Box CM, Duke Station Durham, North Carolina 27706 Attn: Metallurgy & Ceramics Division	1
Army Materials and Mechanics Research Center Watertown, Massachusetts 02172 Attn: Research Programs Office (AMXMR-P)	1

UNCLASSIFIED
NSWC/WOL/TR 76-99

DIST. Cont.

Copies

Air Force Office of Scientific Research Building 410 Bolling Air Force Base Washington, D. C. 20332 Attn: Chemical Science Directorate Electronics and Solid State Sciences Directorate	1 1
Air Force Materials Lab (LA) Wright-Patterson Air Force Base Dayton, Ohio 45433	1
NASA Headquarters Washington, D. C. 20546 Attn: Code RRM	1
NASA Lewis Research Center 21000 Brookpark Road Cleveland, Ohio 44135 Attn: Library	1
National Bureau of Standards Washington, D. C. 20234 Attn: Metallurgy Division Inorganic Materials Division	1 1
Defense Metals and Ceramics Information Center Battelle Memorial Institute 505 King Avenue Columbus, Ohio 43201	1
Director Ordnance Research Laboratory P. O. Box 30 State College, Pennsylvania 16801	1
Director Applied Physics Laboratory University of Washington 1013 Northeast Fortieth Street Seattle, Washington 98105	1

UNCLASSIFIED
NSWC/WOL/TR 76-99

DIST. Cont.

	Copies
Metals and Ceramics Division Oak Ridge National Laboratory P. O. Box X Oak Ridge, Tennessee 37380	1
Los Alamos Scientific Laboratory P. O. Box 1663 Los Alamos, New Mexico 87544 Attn: Report Librarian	1
Argonne National Laboratory Metallurgy Division P. O. Box 229 Lemont, Illinois 60439	1
Technical Information Division Upton, Long Island New York 11973 Attn: Research Library	1
Lawrence Radiation Laboratory Building 50 Room 134 Berkeley, California 94720 Attn: Library	1
Professor G. S. Ansell Rensselaer Polytechnic Institute Department of Metallurgical Engineering Troy, New York 12181	1
Professor H. D. Brody University of Pittsburgh School of Engineering Pittsburgh, Pennsylvania 15213	1
Professor J. B. Cohen Northwestern University Department of Material Sciences Evanston, Illinois 60201	1
Professor M. Cohen Massachusetts Institute of Technology Department of Metallurgy Cambridge, Massachusetts 02100	1
Professor B. C. Giessen Northeastern University Department of Chemistry Boston, Massachusetts 02115	1

UNCLASSIFIED
NSWC/WOL/TR 76-99

DIST. Cont.

Dr. G. T. Hahn Battelle Memorial Institute Department of Metallurgy 505 King Avenue Columbus, Ohio 43201	1
Professor R. W. Heckel Carnegie-Mellon University Schenley Park Pittsburgh, Pennsylvania 15213	1
Professor R. F. Hehemann Case Western Reserve University Department of Metallurgy & Materials Science Cleveland, Ohio 44106	1
Professor G. Judd Rensselaer Polytechnic Institute Department of Materials Engineering Troy, New York 12181	1
Professor A. Lawley Drexel University Department of Metallurgical Engineering Philadelphia, Pennsylvania 19104	1
Professor R. Maddin University of Pennsylvania School of Metallurgical Engineering Philadelphia, Pennsylvania 19105	1
Professor J. W. Morris, Jr. University of California College of Engineering Berkeley, California 94720	1
Professor R. M. Rose Massachusetts Institute of Technology Department of Metallurgy Cambridge, Massachusetts 02100	1
Professor O. D. Sherby Stanford University Materials Sciences Department Stanford, California 94300	1
Professor J. Shyne Stanford University Materials Sciences Department Stanford, California 94300	1

UNCLASSIFIED
NSWC/WOL/TR 76-99

DIST. Cont.

Professor N. S. Stoloff Rensselaer Polytechnic Institute School of Engineering Troy, New York 12181	1
Dr. E. R. Thompson United Aircraft Research Laboratories 400 Main Street East Hartford, Connecticut 06108	1
Professor David Turnbull Harvard University Division of Engineering & Applied Physics Cambridge, Massachusetts 02100	1
Professor H. G. F. Wilsdorf University of Virginia Department of Materials Science Charlottesville, Virginia 22903	1
Dr. J. C. Williams Rockwell International Science Center P. O. Box 1085 Thousand Oaks, California 91360	1
Professor D. A. Koss Michigan Technological University College of Engineering Houghton, Michigan 49931	1
Dr. E. A. Starke, Jr. Georgia Institute of Technology School of Chemical Engineering Atlanta, Georgia 30332	1
Dr. W. A. Spitzig U.S. Steel Corporation Research Laboratory Monroeville, Pennsylvania 15146	1
Dr. M. A. Wright University of Tennessee Space Institute Department of Metallurgical Engineering Tullahoma, Tennessee 37388	1

UNCLASSIFIED
NSWC/WOL/TR 76-99

DIST. Cont.

Dr. L. Leonard The Franklin Institute Research Laboratories The Benjamin Franklin Parkway Philadelphia, Pennsylvania 19103	1
Professor L. E. Murr New Mexico Institute of Mining & Technology Metallurgical Engineering Socorro, New Mexico 87801	1
Dr. G. H. Meier University of Pittsburgh Department of Metallurgical & Materials Engineering Pittsburgh, Pennsylvania 15213	1
Dr. J. R. Low, Jr. Carnegie-Mellon University Metals Research Laboratory Schenley Park Pittsburgh, Pennsylvania 15213	1
Professor H. K. Birnbaum University of Illinois Department of Metallurgy Urbana, Illinois 61801	1
Dr. C. S. Kortovich TRW, Incorporated 23555 Euclid Avenue Cleveland, Ohio 44117	1

TO AID IN UPDATING THE DISTRIBUTION LIST
FOR NAVAL SURFACE WEAPONS CENTER, WHITE
OAK LABORATORY TECHNICAL REPORTS PLEASE
COMPLETE THE FORM BELOW:

TO ALL HOLDERS OF NSWC/WOL/TR 76-99
by A. E. Clark, Code WR-34
DO NOT RETURN THIS FORM IF ALL INFORMATION IS CURRENT

A. FACILITY NAME AND ADDRESS (OLD) (Show Zip Code)

NEW ADDRESS (Show Zip Code)

B. ATTENTION LINE ADDRESSES:

C.

REMOVE THIS FACILITY FROM THE DISTRIBUTION LIST FOR TECHNICAL REPORTS ON THIS SUBJECT.

D.

NUMBER OF COPIES DESIRED _____

**DEPARTMENT OF THE NAVY
NAVAL SURFACE WEAPONS CENTER
WHITE OAK, SILVER SPRING, MD. 20910**

**OFFICIAL BUSINESS
PENALTY FOR PRIVATE USE, \$300**

**POSTAGE AND FEES PAID
DEPARTMENT OF THE NAVY
DOD 316**



**COMMANDER
NAVAL SURFACE WEAPONS CENTER
WHITE OAK, SILVER SPRING, MARYLAND 20910**

ATTENTION: CODE WR-34

FILM
5